Microporous Mg−Si−O and Al−Si−O Materials Derived from Metal Silsesquioxanes

Nicolae Maxim,[†] Pieter C. M. M. Magusin,[†] Patricia J. Kooyman,[‡] Jos H. M. C. van Wolput,[†] Rutger A. van Santen,[†] and Hendrikus C. L. Abbenhuis*,[†]

Schuit Institute of Catalysis, Eindhoven University of Technology, P.O. Box 513, 5600 MB Eindhoven, The Netherlands and National Centre for HREM Delft, Rotterdamseweg 137, 2628 AL Delft, The Netherlands

Received March 29, 2001. Revised Manuscript Received June 29, 2001

Microporous amorphous metallosilicates designated as Mg−Si−O and Al−Si−O, with a very narrow pore size distribution around 6 Å diameter, typical surface areas ranging from 350 to 650 m^2/g, and loadings of well-dispersed metal oxide (up to about 10 wt % metal) result from the controlled calcination of magnesium and aluminum silsesquioxane complexes $[(c\text{-}C_5H_9)_7Si_7O_{12}]_2Mg_4Cl_2 \cdot 2THF$, **1**, $\{[(c\text{-}C_5H_9)_7Si_7O_{12}]Al\}_n$, **2**, and $[(c\text{-}C_5H_9)_7Si_7O_{11}(OSiMe_3)]$-$Al[(c\text{-}C_5H_9)_7Si_7O_{10}(OSiMe_3)(OH)]$, **3**. Moreover, textural properties such as surface area and pore volume can be easily adjusted by varying the calcination conditions, while the pore size distribution remains practically unchanged. XPS, EDX, solid-state MAS ^{29}Si and ^{27}Al NMR, and HRTEM measurements suggest that the metal is present in M−Si−O materials mainly as isolated metal ions incorporated in the amorphous silica framework and also as small crystalline metal oxide particles of a few nanometers, which are well dispersed throughout the silica. SEM was employed as well to evaluate particle size and morphology. IR spectroscopy of adsorbed acetonitrile showed that both Al−Si−O materials are strong Lewis acids. Mg−Si−O and Al−Si−O were briefly tested as catalysts in 1-butanol dehydration. Mg−Si−O gave both dehydrogenation and dehydration, while on Al−Si−O only dehydration and cracking reactions occurred.

Introduction

Silsesquioxane chemistry spans more than half a century, but the interest in this field has increased dramatically over the past decade due to the applications of these compounds in materials science and catalysis. Silsesquioxanes have been found to be useful precursors for ceramic materials,[1] while metallasilsesquioxanes have attracted attention from the viewpoint of well-defined homogeneous models for the active surface sites of supported catalysts or metal-containing zeolites.[2] Moreover, titanium-containing silsesquioxanes are active catalysts for epoxidation of olefins[3] while titanium- or zirconium-containing silsesquioxanes have been reported to be active catalysts for olefin polymerization.[4]

Recent studies focus on the application of metal-containing silsesquioxanes as convenient precursors for microporous amorphous M−Si−O materials.[5] These materials are characterized by a high surface area, uniformly controlled micropores, and good metal dispersion, being therefore potential heterogeneous catalysts. This development has also been stimulated by the fact that over the past decade a large number of metal silsesquioxane complexes have become available. Nowadays, the metals incorporated into the Si/O skeleton of silsesquioxanes include main group, early, and late transition metals, as well as chalcogens:[6] Li, Na, Mg, Y, La, Ti, Zr, Hf, V, Cr, Mo, W, Fe, Os, Pt, Zn, B, Al, Ga, Tl, Ge, Sn, P, Sb, Te. The known literature involves the calcination of titanium and chromium silsesquioxanes in order to form microporous mixed oxides.[5b,c]

Sol−gel method can also be used to prepare mixed oxides or metal supported on silica. However, homogeneity of the multicomponent gels, in terms of the distribution of various components, strongly affects the

* Corresponding author. E-mail: H.C.L.Abbenhuis@tue.nl.
† Eindhoven University.
‡ National Centre for HREM Delft.

(1) (a) Baney, R. H.; Itoh, M.; Sakakibara, A.; Suzuki, T. *Chem. Rev.* **1995**, *95*, 1409. (b) Agaskar, P. A. *J. Chem. Soc., Chem. Commun.* **1992**, 1024.

(2) (a) Feher, F. J.; Budzichowski, T. A. *Polyhedron* **1995**, *14*, 3239.

(3) (a) Maschmeyer, T.; Klunduk, M. C.; Martin, C. M.; Shephard, D. S.; Thomas, J. M.; Johnson, B. F. G. *Chem. Commun.* **1997**, 1847. (b) Crocker, M.; Herold, R. H. M.; Orpen, A. G. *Chem. Commun.* **1997**, 2411.

(4) (a) Duchateau, R.; Abbenhuis, H. C. L.; van Santen, R. A.; Meetsma, A.; Thiele, S. K. H.; van Tol, M. F. H. *Organometallics* **1998**, *17*, 5663. (b) Duchateau, R.; Cremer, U.; Harmsen, R. J.; Mohamud, S. I.; Abbenhuis, H. C. L.; van Santen, R. A.; Meetsma, A.; Thiele, S. K. H.; van Tol, M. F. H.; Kranenburg, M. *Organometallics* **1999**, *18*, 5447.

(5) (a) Wada, K.; Nakashita, M.; Yamamoto, A.; Mitsudo, T. *Chem. Commun.* **1998**, 133. (b) Wada, K.; Nakashita, M.; Bundo, M.; Ito, K.; Kondo, T.; Mitsudo, T. *Chem. Lett.* **1998**, 659. (c) Maxim, N.; Abbenhuis, H. C. L.; Stobbelaar, P. J.; Mojet, B. L.; van Santen, R. A. *Phys. Chem. Chem. Phys.* **1999**, *18*, 4473. (d) Wada, K.; Bundo, M.; Nakabayashi, D.; Itayama, N.; Kondo, T.; Mitsudo, T. *Chem. Lett.* **2000**, 628.

(6) (a) Voronkov, M. G.; Lavrent'yev, V. I. *Top. Curr. Chem.* **1982**, *102*, 199. (b) Lorenz, V.; Fischer, A.; Giebmann, S.; Gilje, J. W.; Gun'ko, Y.; Jacob, K.; Edelmann, F. T. *Coord. Chem. Rev.* **2000**, *206−207*, 321. (c) Abbenhuis, H. C. L. *Chem. Eur. J.* **2000**, *6*, 25.

10.1021/cm010272g CCC: $20.00
Published on Web 08/29/2001

properties of the final oxide.[7] For example, in the TiO_2−SiO_2 gel, titanium alkoxide hydrolyzes much faster than silicon akoxide. Thus, hydrolysis of a liquid mixture of the two alkoxides would eventually result in the formation of titanium oxyhydroxide clusters imbedded in the silica gel, and segregation of TiO_2 and SiO_2 after calcination.[8]

The use of the metal silsesquioxane precursors guarantees that the metal and silicon are atomically mixed. Assuming that the water formed during calcination causes only minor hydrolysis of the M−O−Si bonds and that the hydrolyzed metal species have low mobility, then a uniform distribution of the metal throughout the silica is expected.

Thus, as described previously for chromium silsesquioxane, during calcination the organic groups attached to the silicon atoms are replaced by Si−O−Si linkages that seem to connect the initially isolated Si/O-cage structures. The resulting amorphous material had a very narrow pore size distribution centered at 6 Å. A relatively high loading (about 10 wt % metal) of monodispersed metal oxide could be realized as well.[5c]

We have started a detailed investigation into the use of silsesquioxane metal complexes as precursors for porous metallosilicates. In this paper, we access aspects of this new methodology that are relevant to the area of catalysis. These involve the optimization and scope of the method of calcination and evaluation of the possibility to adjust the texture of metallosilicates and their metal dispersion by changing the calcination conditions.

Complex **3** can be considered as a model for a Brønsted acidic zeolite site, while complex **2** has aluminum sites that are exclusively Lewis acidic.[9] It was reported that solid acidic catalysts active for 1-butene isomerization have been prepared from the silsesquioxane triol, $(c\text{-}C_5H_9)_7Si_7O_9(OH)_3$, deposited on alumina surface followed by calcination in air.[10] Therefore, we examined also the possibility of preparing metallosilicates that are exclusively Lewis or Brønsted acids.

To develop and assess this methodology, the known magnesium and aluminum silsesquioxane complexes **1**−**3** were used (see Figure 1).[9,11]

The M−Si−O materials resulting from calcination of compounds **1**, **2**, and **3** were carefully characterized with regard to both the textural properties and the metal state and dispersion by the use of a set of different complementary techniques including nitrogen physical adsorption, XRD, XPS, EDX, solid-state MAS ^{29}Si and ^{27}Al NMR, HRTEM, and SEM.

Experimental Section

Synthesis of the M−Si−O Materials. The magnesium silsesquioxane complex **1** was prepared by reacting the trisilanol silsesquioxane[12] $(c\text{-}C_5H_9)_7Si_7O_9(OH)_3$ with the Grignard reagent CH_3MgCl in THF solvent.[11] The aluminum silsesquioxane complexes **2** and **3** were prepared by reacting $AlEt_3$ with this trisilanol silsesquioxane in THF and disilanol silsesquioxane[13] $(c\text{-}C_5H_9)_7Si_7O_9(OSiMe_3)(OH)_2$ in toluene, respectively.[9] Structures of magnesium and aluminum silsesquioxane complexes were verified by using ^1H and ^{13}C NMR as well as solid-state MAS ^{29}Si NMR.

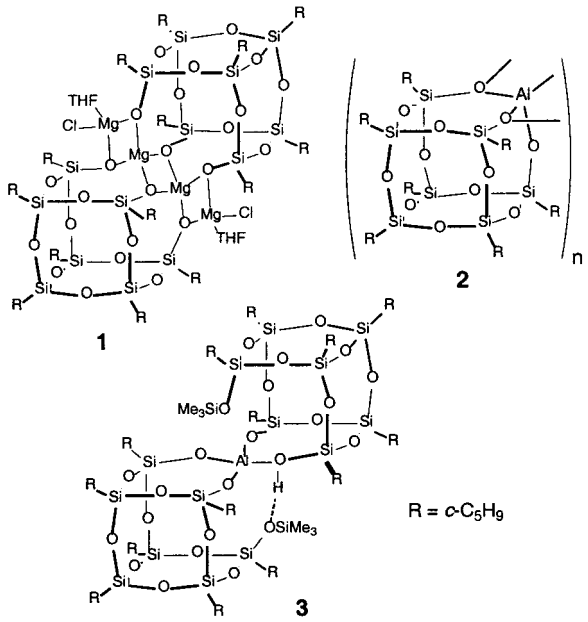

Figure 1. Magnesium and aluminum silsesquioxane complexes **1**−**3** (R = C_5H_9).

Small portions of 0.5 g of metal-containing oligosilsesquioxane **1**, **2**, and **3** as well as metal-free silsesquioxane $(c\text{-}C_5H_9)_7Si_7O_9(OH)_3$ were heated at 5 °C min^{-1} to 500 °C for 4 h in a continuous plug-flow reactor of 27 mm internal diameter flushed by an Ar−O_2 gas mixture flow of 30 mL/min containing 20 mol % O_2. As reported earlier for calcination of chromium silsesquioxane, these conditions allowed an efficient carbon removal and led to large surface area materials.[5c] The resultant oxides are further designated as Mg−Si−O, Al−Si−O(I), Al−Si−O(II), and SiO_2. For calcination conditions other than the standard ones mentioned above, additional suffixes are used for designations (e.g., Mg−Si−O-425 °C means that the sample was calcined at 425 instead of 500 °C but the gas flow and the calcination time were standard). The M−Si−O metal content, as calculated, is 9.7 wt % for Mg−Si−O, 5.7 wt % for Al−Si−O(I), and 2.6 wt % for Al−Si−O(II).

Analysis. The carbon content of the M−Si−O materials was measured by heating the samples at 925 °C on a Perkin-Elmer automated analyzer Series II CHNS/O Analyzer 2400.

For nitrogen physisorption analysis, all samples were pretreated before the measurement in a vacuum at 200 °C for 2 h. The measurements were performed on Micromeritics ASAP 2000 using an equilibriation interval of 5 s and a low pressure dose of 3.00 cm^3/g STP. Surface area, pore volume, and pore size distribution were calculated using the methods developed by Horvath−Kawazoe and Dubinin−Radushkevich.[14]

X-ray diffraction (XRD) data were collected on a Rigaku diffractometer in the range $5.0° < 2\theta < 80°$ using Cu Kα radiation and the step scan method at 0.1 deg/min scanning speed and 5 s dwelling time.

X-ray photoelectron spectroscopy (XPS) measurements were done using a VG CLAM 2 spectrometer equipped with a Mg Kα source and a hemispherical analyzer. Measurements were

(7) Kung, H. H.; Ko, E. I. *Chem. Eng. J.* **1996**, *64*, 203.
(8) Hutter, H.; Mallat, T.; Baiker, A. *J. Catal.* **1995**, *153*, 177.
(9) Duchateau, R.; Harmsen, R. J.; Abbenhuis, H. C. L.; van Santen, R. A.; Meetsma, A.; Thiele, S. K.-H.; Kranenburg, M. *Chem. Eur. J.* **1999**, *5*, 3130.
(10) Imizu, Y.; Takahara, K.; Okazaki, N.; Itoh, H.; Tada, A.; Ohnishi, R.; Ichikawa, M. *Stud. Surf. Sci. Catal.* **1994**, *90*, 339.
(11) Hanssen, R. W. J. M.; Meetsma, A.; van Santen, R. A.; Abbenhuis, H. C. L. *Inorg. Chem.* **2001**, *40*, 4049.
(12) Feher, F. J.; Budzichowski, T. A.; Blanski, R. L.; Weller, K. J.; Ziller, J. W. *Organometallics* **1991**, *10*, 2526.
(13) Abbenhuis, H. C. L.; Burrows, A. D.; Kooijman, H.; Lutz, M.; Palmer, M. T.; van Santen, R. A.; Spek, A. L. *Chem. Commun.* **1998**, 2627.
(14) (a) Dubinin, M. M.; Radushkevich, L. V. *Proc. Acad. Sci. USSR* **1947**, *55*, 331. (b) Horwath, G.; Kawazoe, K. *J. Chem. Eng. Jpn.* **1983**, *16*, 470.

carried out at 20 eV pass energy. Charging was corrected by using the Si 2p peak of SiO_2 at 103.3 eV. The samples were ground and pressed in indium foil which was placed on a stainless steel stub. The XP spectra have been fitted with a VGS program fit routine, with a Shirley background subtraction and Gauss−Lorentz curves. The error in the binding energy was 0.2 eV. Elemental ratios were calculated from the peak areas with correction for the cross sections.[15]

Energy-dispersive X-ray (EDX) elemental analysis was performed using a JEOL SUPERPROBE JXA-8600SX at an accelerating voltage of 10 kV. The powder samples were coated with carbon before measurement in order to create a conductive film (about 25 nm thickness) at the sample surface. The probe spot size was about 40 nm.

Solid-state magic-angle-spinning (MAS) ^{29}Si nuclear magnetic resonance (NMR) experiments were carried out on a Bruker MSL400 spectrometer operating at a ^{29}Si resonance frequency of 79.46 MHz. The peak of Q8M8 at 11.8 ppm was used as an external reference for the chemical shift. Magic-angle spinning at a sample rotation rate of 4 kHz was employed to eliminate the line broadening caused by the chemical shift anisotropy. Chemical shift values were estimated from MAS ^{29}Si NMR spectra recorded with direct ^{29}Si excitation combined with high-power proton decoupling and relaxation delays of 30 s between subsequent scans. (Longer relaxation delays up to 300 s did not yield line shape changes.) Typically 64−128 scans were recorded. MAS ^{27}Al NMR spectra were obtained on a Bruker DMX500 operating at a ^{27}Al NMR frequency of 130.32 MHz. A MAS rate of 12.5 kHz was employed, and an echo synchronized with the sample rotation was recorded at $2\tau = 160\ \mu s$. The repetition time was 1 s, and the number of scans was 6400.

Transmission electron microscopy (TEM) was performed using a STEM JEOL 2000 FX transmission electron microscope operated at 120 kV and a Philips CM30UT high-resolution electron microscope with a field emission gun as a source of electrons operated at 300 kV. Samples were mounted on a microgrid carbon polymer supported on a copper grid by placing a few droplets of a suspension of ground sample in ethanol on the grid followed by drying at ambient conditions.

Scanning electron microscopy (SEM) images were taken with a field emission gun (FEG) XL30 instrument operated at an accelerating voltage of 10 kV.

IR spectra were measured on a Bruker FTIR spectrometer (IFS 113v) equipped with a vacuum cell. Self-supporting disks with a thickness of 8 $mg \cdot cm^{-2}$ were used. The spectra were recorded by co-adding 500 scans at room temperature with a resolution of 4 cm^{-1}. Activation of the samples was performed at 720 K in a high vacuum (10^{-6} mbar) for 2 h. After cooling to room temperature, the spectrum of the unloaded sample was taken, followed by contacting the sample with deuterated acetonitrile for 30 min at a presure of 0.9 mbar and recording of a new spectrum. After this, the loading of the samples was reduced stepwise by lowering the equilibrium pressure to 0.05 mbar as well as by desorption for 30 min at 298, 353, and 573 K, respectively, followed by collecting room-temperature spectra after each step. The spectrum of the unloaded sample was subtracted from the spectra of samples with different acetonitrile loadings.

Mg−Si−O and Al−Si−O samples were tested in 1-butanol dehydration. Catalytic tests were performed in a continuous plug-flow reactor at 200 and 300 °C using 0.7 g of catalyst. The reaction products were analyzed by gas chromatographic methods.

Results and Discussion

Since the calcined magnesium and aluminum silsesquioxane complexes as well as the calcined silsesquioxane triol were brownish in color, indicating the presence of residual carbon in the M−Si−O materials, we measured the carbon content. The effect of O_2 flow, calcination time, and calcination temperature on residual carbon content in Mg−Si−O materials is shown in Figure 2. Obviously the residual carbon removal can be improved by changing the calcination conditions. At low calcination temperature (425 °C) and 4 h calcination time, the higher the O_2 flow the lower the residual C content. An increase in calcination time from 4 to 16 h significantly diminishes the residual percentage of C, but the effect of the O_2 flow becomes negligible. However, the most important factor seems to be the calcination temperature; high temperatures are necessary for complete carbon removal. Thus, a calcination temperature of 500 °C led to a Mg−Si−O material with a surface area of 347 m^2/g and only 0.6 wt % C. Of course calcination temperatures as high as 550 °C can be used, but higher temperatures may significantly decrease the surface area and pore volume of the samples. It has been reported that for an oligomeric silsesquioxane−siloxane copolymer the use of pyrolysis temperatures above 600 °C led to materials with a reduced surface area.[16] As described in this reference, the porosity, surface area, and density measurements showed that char densification took place after the majority of mass loss from pyrolysis had occurred. Once the maximum density had been reached, pore closure occurred between 600 and 650 °C and the surface area decreased from 406 to 2.5 m^2/g. Therefore, appropriate temperatures for the calcination of the metallasilsesquioxane precursors range from 500 to 550 °C.

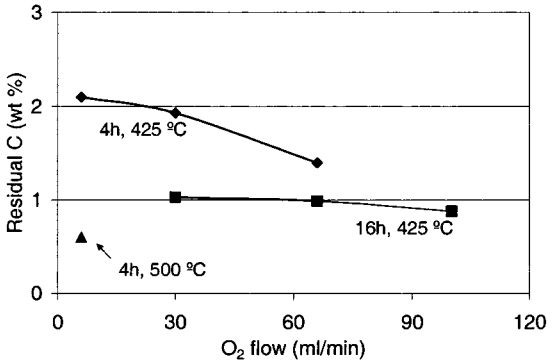

Figure 2. Effect of calcination conditions on the residual carbon content of M−Si−O materials (exemplified for Mg−Si−O).

Typical values for surface area, pore volume, and average pore diameter for Mg−Si−O and Al−Si−O as well as for SiO_2-450 °C materials that were derived from N_2 physisorption isotherms are presented in Table 1. These results indicate the formation of microporous materials characterized by high surface area, rather large pore volume, and a very narrow pore size distribution with an average pore size diameter around 6−7 Å.

As reported earlier, the surface area and pore volume of the M−Si−O materials depended on the calcination temperature.[5b,c] Therefore, for optimization of the proposed methodology here, we have tried different calcination conditions to determine if it is possible to adjust the texture of the metallosilicates and their metal dispersion. Calcination conditions which have been

(15) Scofield, J. H. *J. Electron Spectrosc. Relat. Phenom.* **1976**, *8*, 129.

(16) Mantz, R. A.; Jones, P. F.; Chaffee, K. P.; Lichtenhan, J. D.; Gilman, J. W. *Chem. Mater.* **1996**, *8*, 1250.

Table 1. Nitrogen Sorption Data for Mg−Si−O, Al−Si−O, and SiO_2

sample	surf. area[a] (m^2/g)	pore vol[b] (mL/g)		av pore diam[c] (Å)
Mg−Si−O	347	0.12	0.12	6.0
Al−Si−O(I)	583	0.20	0.19	6.4
Al−Si−O(II)	641	0.22	0.21	6.3
SiO_2-450 °C	499	0.17	0.17	6.1

[a] Estimated from Dubinin−Radushkevich equation. [b] Estimated from Dubinin−Radushkevich (first column) and Horvath−Kawazoe equations (second column). [c] Estimated from Horvath−Kawazoe equation.

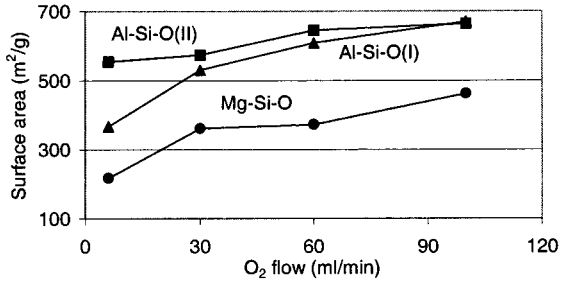

Figure 3. Effect of O_2 flow on the surface area of Mg−Si−O, Al−Si−O(I), and Al−Si−O(II) materials.

tested included temperature, which was varied in the range 425−550 °C; pure O_2 flows of 6−100 mL/min; a 30 mL/min flow of 20 mol % O_2 in Ar; and a calcination time of either 4 or 16 h.

Thus, the surface area of M−Si−O materials can be greatly changed by altering the O_2 flow, as we show in Figure 3 for Mg−Si−O, Al−Si−O(I), and Al−Si−O(II). The surface area of all the samples increased with the O_2 flow. The lower surface areas for the Mg−Si−O sample might be attributed to a sintering process promoted by the water resulting from combustion of the organic part of silsesquioxane complex. It was reported that the surface area of active magnesia prepared by calcination procedures is significantly diminished due to sintering in the presence of water vapors. The greater effect of water on the sintering rate of magnesia compared with alumina and silica was attributed to the low charge and correspondingly high mobility of the magnesium ions.[17] The difference found between the surface area of two batches of M−Si−O calcined under the same conditions was below 8%, indicating a rather good reproducibility of the data presented in Figure 3.

There is also a significant temperature effect, since an increase in temperature from 425 to 475 °C diminished the Mg−Si−O surface area by ca. 25% and reduced the carbon content by ca. 63%. From this point of view relatively low calcination temperatures are required in order to obtain high surface areas.

A longer calcination time can be effective for reducing the residual carbon content, especially at low temperatures such as 425 °C, but it can also decrease significantly the surface area. However, at higher calcination temperatures of at least 500 °C, a 4 h calcination time seems to be enough to remove the carbon almost completely from all the M−Si−O materials while large surface areas are obtained.

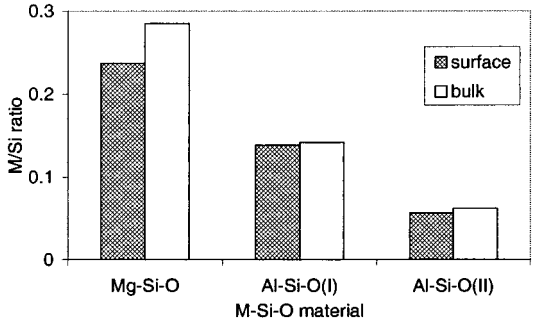

Figure 4. Comparison of bulk and surface (XPS data) M/Si atomic ratios for Mg−Si−O, Al−Si−O(I), and Al−Si−O(II) materials.

Pure O_2 flows can more efficiently remove residual carbon than diluted O_2 flows. They usually have little effect on textural properties of M−Si−O materials in comparison with Ar-diluted O_2 flows, but sometimes they can prevent mesopore formation. When an Ar-diluted O_2 flow was used, all of the M−Si−O samples, excepting the Al−Si−O(I), yielded type Ib isotherms characteristic of microporous materials. Al−Si−O(I) afforded a type IIb curve associated with a steep increase in the adsorption amount at low p/p_0, indicative for the presence of both micro- and mesopores. When we used pure O_2, the isotherm was type Ib as well. Attribution of the M−Si−O material isotherms was made according to extended IUPAC classification.[18]

Whereas the surface area and pore volume can be adjusted rather well by changing the calcination conditions, the pore size distribution does not change significantly. However, since textural properties such as surface area are very sensitive to the calcination conditions, the latter ones must be well controlled in order to achieve good reproducibility. For comparison, we chose a calcination temperature of 500 °C, a calcination time of 4 h, and an Ar-diluted O_2 flow of 30 mL/min 20% O_2 as standard conditions.

The metal dispersion and state for Mg−Si−O and Al−Si−O materials were investigated by XPS, EDX, MAS ^{29}Si and ^{27}Al NMR, and TEM techniques.

If we assume that all of the metal species are homogeneously distributed throughout the M−Si−O materials, then the surface and the bulk ratios should be similar. The M/Si atomic ratios calculated from the composition of silsesquioxane complexes **1**, **2**, and **3** are 0.285, 0.142, and 0.062, respectively. These bulk M/Si ratios are compared in Figure 4 with the surface M/Si ratios determined by XPS analysis. The surface and bulk M/Si ratios are almost the same for the Mg−Si−O and the Al−Si−O materials, indicating a rather high dispersion of the metal throughout the silica and on its surface.

The homogeneity of the metal distribution inside the M−Si−O materials was also estimated from EDX spectra. It is known that emitted X-rays are characteristic for an element and that measuring their intensities allows the quantification of the chemical composition of a selected part of the sample. Thus we measured the composition of Mg−Si−O and Al−Si−O in five different

(17) (a) Anderson, P. J.; Morgan, P. L. *Trans. Faraday Soc.* **1964**, *60*, 930. (b) Adams, C. R. *J. Phys. Chem.* **1963**, *67*, 313. (c) Schlaffer, W. G.; Morgan, C. Z.; Wilson, J. N. *J. Phys. Chem.* **1957**, *61*, 714. (d) Shapiro, I.; Kolthoff, I. M. *J. Am. Chem. Soc.* **1950**, *72*, 776.

(18) Rouquerol, F.; Rouquerol, J.; Sing, K. *Adsorption by Powders & Porous Solids—Principles, Methodology and Applications*; Academic Press: London, 1999.

Table 2. Solid-State MAS ^{29}Si NMR Chemical Shift for Mg−Si−O, Al−Si−O, and SiO_2

material	$-\delta$ (ppm)
Mg−Si−O[a]	105.44
SiO_2[a]	109.50
SiO_2[a] + MgO (physical mixture)	109.50
Al−Si−O(I)[b]	104.89
Al−Si−O(II)[b]	105.81
SiO_2[b]	108.76

[a] Samples calcined at 425 °C/16 h/30 mL·min^{-1} O_2. [b] Samples calcined at 500 °C/4 h/30 mL·min^{-1} 20%O_2 in Ar (standard conditions).

randomly selected areas of the samples, using a probe spot size of about 40 nm. The found M/Si atomic ratios are fairly close to the expected bulk ratios, indicating also a rather good distribution of the metal species inside the samples even if this distribution is not fully homogeneous.

It should be noted also that the XPS Al/Si ratio for Al−Si−O(I) did not change significantly when different O_2 flows in the range 6−100 mL/min were used, indicating a rather stable dispersion of aluminum species in the Al−Si−O material.

Solid-state MAS ^{29}Si NMR spectra of the calcined magnesium and aluminum silsesquioxane complexes **1**, **2**, and **3**, as well as of the calcined metal-free silsesquioxane ligand (c-C_5H_9)$_7Si_7O_9(OH)_3$, were recorded. We measured also the spectrum of a physical mixture of calcined metal-free silsesquioxane ligand (c-C_5H_9)$_7Si_7O_9$-$(OH)_3$ and MgO with the same content of Mg as in the Mg−Si−O material. All of these materials show a single, broad ^{29}Si resonance with a clearly defined maximum having a chemical shift value at -105.5 ± 0.5 ppm for M−Si−O materials and around -109.5 ± 0.5 ppm for pure silica, as shown in Table 2. The observed chemical shift for the M−Si−O materials indicates a higher proportion of Q3 than Q4 environment in the second coordination sphere of Si atoms (Q3 stands for MOSi-$(OSi)_3$ and Q4 stands for $Si(OSi)_4$). Thus, we can assume that the metal ions are mainly incorporated into the amorphous silica framework formed during the calcination process. Moreover, the physical mixture of pure silica and magnesium oxide presents the same chemical shift as pure silica. Therefore, the observed shift for the Mg−Si−O cannot be attributed to some susceptibility effect caused by the formation of a separate MgO phase.

Solid-state MAS ^{27}Al NMR spectra of Al−Si−O(I) and Al−Si−O(II) materials, presented in Figure 5, show two well-defined peaks at ca. 0−3 and 52−54 ppm and a broad peak at 30 ppm. The peak at 0−3 ppm is assigned to octahedral Al and that at 52−54 pm to tetrahedral Al.[19] The less defined peak at 30 ppm has been attributed to distorted tetrahedral Al, to five-coordinated Al, or to both.[20] Thus, according to the assignment of the peaks at 52−54 and 30 ppm to tetrahedral and, respectively, distorted tetrahedral and/or pentacoordinated Al sites, NMR data suggest that Al is mainly incorporated in the silica framework. The presence of the octahedral signal at 0 ppm indicates that a significant part of Al is forming small particles of Al_2O_3.

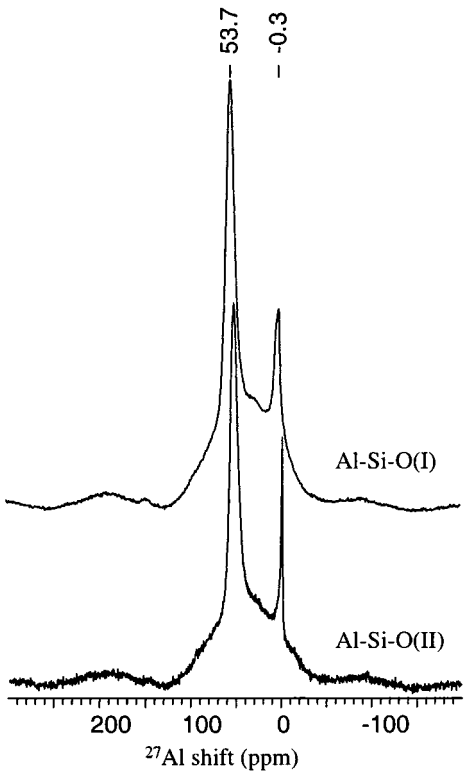

Figure 5. MAS ^{27}Al NMR spectra of Al−Si−O(I) and Al−Si−O(II).

Observing the metal dispersion with transmission electron microscopy requires sufficient contrast between the metal oxide and the support, and it can be difficult to detect small and highly dispersed metal oxide particles on the support surface. Nevertheless, Mg−Si−O and Al−Si−O materials were examined with HRTEM, which allowed us to get good images of thin areas of the samples as shown in Figure 6. In these micrographs well-dispersed darker spots (Figure 6a,c) presenting lattice fringes (Figure 6b) can be seen on the silica surface. The small size of these crystalline particles, around 5 nm, explains why they were not detected by XRD. Since the XRD patterns of the Mg−Si−O and Al−Si−O materials present only a broad band around 20−30° 2θ angle usually assigned to amorphous silica,[21] identification of the nature of these particles is rather difficult. However, the measurements of lattice fringe spacings of the small crystalline phases and comparison with reference XRD data for MgO, Al_2O_3, and several metal silicates indicated that they are more probably metal oxide than metal silicate particles. Thus, we assigned these particles to MgO in Mg−Si−O and to α-Al_2O_3 in Al−Si−O materials. This implies that during the calcination procedure some of the M−O−Si bonds can be hydrolyzed by the water formed from combustion of the organic part of the metal silsesquioxane complex and thus allows the migration of metal species on the nascent silica surface with the final formation of metal oxide particles.

(19) (a) Livage, J.; Babonneau, F.; Chatry, M.; Coury, L. *Ceram. Int.* **1997**, *23*, 13. (b) Okada, K.; Tomita, T.; Kameshima, Y.; Yasumori, A.; MacKenzie, K. J. D. *J. Mater. Chem.* **1999**, *9*, 1307.

(20) (a) Samoson, A.; Lippmaa, E.; Engelhardt, G.; Lohse, U.; Jerschkewitz, H.-G. *Chem. Phys. Lett.* **1987**, *134*, 589. (b) Gilson, J.-P.; Edwards, G. C.; Peters, A. W.; Rajagopalan, K.; Wormsbecher, R. F.; Roberie, T. G.; Shatlock, M. P. *J. Chem. Soc., Chem. Commun.* **1987**, 91. (c) Rocha, J.; Carr, S. W.; Klinowski, J. *Chem. Phys. Lett.* **1991**, *187*, 401. (d) Chen, T.-H.; Wouters, B. H.; Grobet, P. J. *Eur. J. Inorg. Chem.* **2000**, 281.

(21) Real, C.; Alcala, M. D.; Criado, J. M. *J. Am. Ceram. Soc.* **1996**, *79*, 2012.

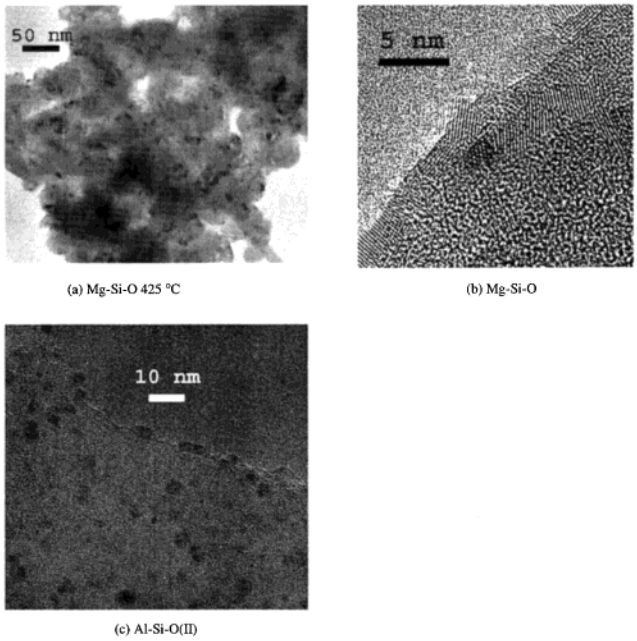

Figure 6. TEM pictures of (a) Mg−Si−O-425 °C, (b) Mg−Si−O, and (c) Al−Si−O(II).

Taking into account the results from XPS, EDX, NMR, and TEM, we can assume that the metal is present in M−Si−O samples mainly as isolated metal ions incorporated in the amorphous silica framework and also as small crystalline metal oxide particles of a few nanometers that are well dispersed throughout silica.

The microtexture of M−Si−O materials was investigated by SEM. The Al−Si−O materials show agglomerates of cubelike particles, while Mg−Si−O and SiO_2 present smooth textures (see Figure 7). The particle size of the ground M−Si−O samples as estimated from SEM images (not shown here for sake of brevity) was roughly 5−20 μm. The aggregates of cube-shaped particles observed for Al−Si−O materials suggest a rather organized structure of these aluminosilicates. However, the XRD and the electron diffraction patterns obtained from Al−Si−O materials indicated only an amorphous phase. For comparison we collected SEM pictures of the noncalcined aluminum silsesquioxane **2** and found only agglomerates of cubelike particles. This indicates that the texture of Al−Si−O materials originates from one of the noncalcined aluminum silsesquioxane precursors which seems to be maintained during calcination.

Complex **3** can be considered as a model for a Brønsted acidic zeolite site, while complex **2** has aluminum sites that are exclusively Lewis acidic. Therefore, we investigated the acid character of the calcined aluminum silsesquioxanes to determine if the resulting metallosilicates are exclusively Lewis or Brønsted acids. Thus, the aluminosilicates resulting from calcination of **2** and **3** were investigated with an in situ IR experiment involving sample treatment with deuterated acetonitrile. As described previously, this provides a good method for discriminating between Lewis and Brønsted acid sites.[22] The CN stretching frequency of CD_3CN can be used efficiently to distinguish between different adsorbing sites on zeolites. IR measurements showed that both Al−Si−O materials possess only Lewis acid sites. Since both Al−Si−O materials gave similar CD_3-CN adsorption spectra, we discuss further only the spectra of Al−Si−O(II) material presented in Figure 8.

When the sample is exposed to CD_3CN gas, a band is observed at 2325 cm^{-1} which is attributed to CD_3CN adsorption on weak Lewis acid sites. When acetonitrile loading is reduced by desorption at 573 K, this band evolves into a less intense one positioned at 2331 cm^{-1} which is assigned to CD_3CN adsorption on strong Lewis acid sites. The band at 2274 cm^{-1} is attributed to the adsorption of CD_3CN on the terminal Si−OH and disappeared after desorption because of the low acidity of this group. The interaction of CD_3CN gas with the terminal Si−OH groups produced also a shift of the Si−OH band from 3742 to 3415 cm^{-1} (not shown here). However, after room-temperature desorption, the Si−OH band came back to 3742 cm^{-1}. No band was practically observed in the 2290−2300 cm^{-1} region indicative of the presence of Brønsted acid sites. Therefore, we conclude that the Brønsted acid sites from **3** are probably converted to Lewis acid sites by dehydration during calcination.

Mg−Si−O, Al−Si−O(I), and Al−Si−O(II) were briefly tested in the dehydrogenation−dehydration reaction of 1-butanol at 200 and 300 °C. On Mg−Si−O, at 200 °C the 1-butanol conversion reached 45% and at 300 °C it became 100%. In the first 30 min at 200 °C, butanal was the main product, but afterward butanal and 1-butene were formed in equal amounts. At 300 °C only dehydration was observed. The color of the catalyst did not change during reaction, suggesting no char building.

Al−Si−O(I) and Al−Si−O(II) were tested under similar conditions and gave at 200 °C 100% conversion. Dehydration to 1-butene is the main reaction that takes place, but also cracking products are present. When the temperature is increased to 300 °C, the cracking reaction becomes predominant. The color of the catalyst turned black during the reaction.

An additional relevant aspect is that we and others[5b,c] find that calcination of metal-free silsesquioxanes also gives rise to the formation of a microporous amorphous silica with a similar pore size distribution. In addition, metallasilsesquioxanes and silsesquioxanes are both soluble in solvents such as tetrahydrofuran. We are now investigating the possibility of adjusting the metal content in M−Si−O materials synthesis by mixing the metal silsesquioxane complex and the metal-free silsesquioxane in THF followed by removal of the solvent and calcination of the solid mixture. This could be a potential route for developing new oxide catalysts, including mixed-metal systems.

Conclusions

Controlled calcination of silsesquioxane metal complexes leads to microporous amorphous metallosilicates with a narrow pore size distribution, high surface area, and high loadings of well-dispersed metal oxide.

Oxidation of organic matter during calcination of the metal silsesquioxane complex precursor leaves a low amount of residual carbon in the resulting M−Si−O materials. The amount of residual carbon can be sig-

(22) (a) Pelmenschikov, A. G.; van Santen, R. A.; Janchen, J.; Meijer, E. *J. Phys. Chem.* **1993**, *97*, 11071. (b) Busio, M.; Jänchen, J.; van Hooff, J. H. C. *Microporous Mater.* **1995**, *5*, 211.

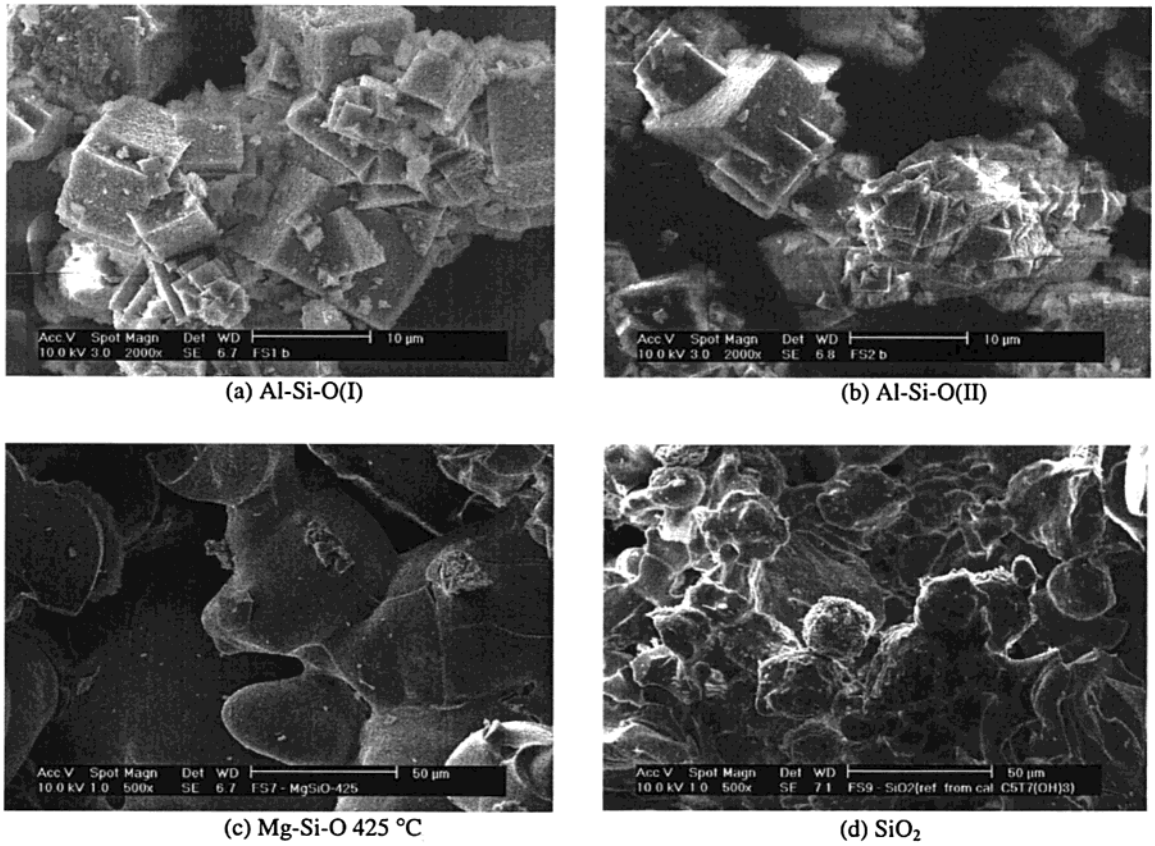

Figure 7. SEM images of (a) Al−Si−O(I), (b) Al−Si−O(II), (c) Mg−Si−O-425 °C, and (d) SiO_2.

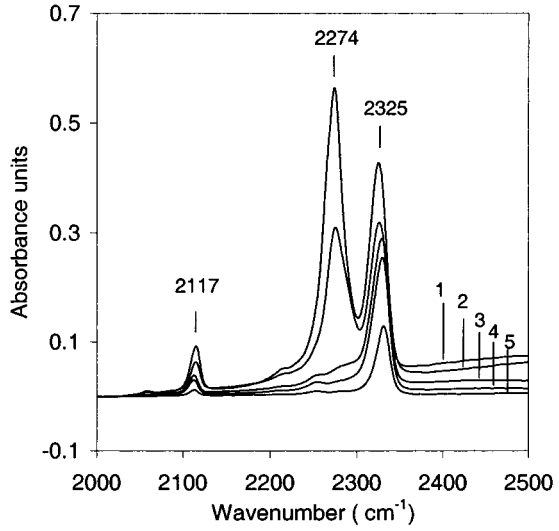

Figure 8. IR spectra of CD_3CN adsorbed on Al−Si−O(II): (1) at 298 K and 0.9 mbar; (2) at 298 K and 0.05 mbar; (3) after desorption at 298 K for 30 min; (4) after desorption at 353 K for 30 min; (5) after desorption at 573 K for 30 min.

nificantly reduced especially by increasing the calcination temperature.

A standard calcination procedure can be generally applied for most of the metal silsesquioxane complex precursors. However, if necessary, calcination conditions such as temperature or O_2 flow can be altered easily in order to adjust the textural properties of the M−Si−O, such as surface area, while retaining the microporous matrix and the pore size distribution.

The spectroscopy and microscopy results show that the metal is present in M−Si−O materials mainly as isolated metal ions incorporated in the amorphous silica framework and also as small crystalline metal oxide particles of a few nanometers that are well dispersed throughout the silica and on its surface.

IR spectroscopy showed that both Al−Si−O materials possess only Lewis acid sites, both weak and strong, therefore leading to the conclusion that the Brønsted sites from **3** are converted to Lewis acid sites probably by dehydration during the calcination procedure.

Mg−Si−O and Al−Si−O were very active in 1-butanol conversion even at 200 °C. Mg−Si−O gave both dehydrogenation and dehydration while on Al−Si−O only dehydration and cracking reactions occurred.

The textural properties and metal dispersion make these M−Si−O materials promising mixed oxide catalysts. Forthcoming results will allow us to evaluate and possibly set up a new tool for synthesis of amorphous mixed oxide catalysts containing more than one metal.

Acknowledgment. This work was supported in part (N.M., P.J.K.) by the Council for Chemical Sciences of The Netherlands Organization for Scientific Research (NWO-CW). Dr. L. Coulier is gratefully acknowledged for his support with the XPS and Mr. E. van Oers for the NMR experiments. Professor J. Th. M. de Hosson is acknowledged for his support with the SEM and Ing. N. J. H. G. M. Lousberg for EDX measurements.

Supporting Information Available: Figure of Si/M molar ratios for M−Si−O materials obtained by EDX and table of lattice fringe spacings found (TEM) for crystallites present in Mg−Si−O and Al−Si−O materials (PDF). This material is available free of charge via the Internet at http://pubs.acs.org.

CM010272G